Available online at www.sciencedirect.com
SCIENCE DIRECT®
Journal of Solid State Chemistry 173 (2003) 59–68
JOURNAL OF SOLID STATE CHEMISTRY
http://elsevier.com/locate/jssc

Comparison between electron–phonon coupling strengths of U^{3+} and Nd^{3+} ions doped in $LaCl_3$ and U^{3+} in $LaBr_3$ single crystals

M. Karbowiak, M. Sobczyk, and J. Drożdżyński*

Department of Chemistry, University of Wrocław, ul. F. Joliot-Curie 14, Wroclaw 50-383, Poland

Received 5 September 2002; received in revised form 13 January 2003; accepted 18 January 2003

Abstract

Temperature-dependent line width and line shift measurements between 7 and 280 K have been performed for a number of absorption transitions in the 4000–21,000 cm^{-1} energy range of the U^{3+}:$LaCl_3$, Nd^{3+}:$LaCl_3$ and U^{3+}:$LaBr_3$ single crystal spectra. The values of the electron–phonon coupling parameter $\bar{\alpha}$ were determined for U^{3+}:$LaCl_3$ and Nd^{3+}:$LaCl_3$ by a fit of experimentally observed line widths to an equation containing the temperature dependent broadening due to the Raman two-phonon process. For both ions diluted in $LaCl_3$ the values of the $\bar{\alpha}$ parameters are considerably lower than in K_2LaCl_5, and the value of $\bar{\alpha}$ for U^{3+} in the $LaCl_3$ host is markedly larger as compared with that of Nd^{3+}. Factors influencing these differences are discussed. With a temperature increase a blue shift of the absorption lines of the U^{3+} ions in $LaCl_3$ and $LaBr_3$ is observed. A comparison has been performed among the electron–phonon coupling parameters obtained from an analysis of the line widths of the U^{3+}:$LaCl_3$ single crystal and those determined from temperature induced line shifts as well as between the magnitudes of the absolute increase in line width and line shifts in the 7–290 K temperature range for U^{3+} doped $LaCl_3$ and $LaBr_3$ crystals. The electron–phonon coupling is stronger for U^{3+} in the tribromide as compared with the trichloride host which is mainly due to a larger covalency of the first one.

Keywords: Electron–phonon coupling; Lanthanides; Actinides; Nd^{3+}; U^{3+}; $LaCl_3$; $LaBr_3$; K_2LaCl_5; Line broadening; Line shifts

1. Introduction

The electron–phonon (EP) coupling in lanthanide ions has been the subject of a considerable number of studies presented, among others, in Refs. [1–6]. For the intraconfigurational $4f^N$ transitions the coupling is relatively weak due to the shielding of the $4f$ electrons by the filled outer $5s^2$ and $5p^6$ shells. For d–d transitions, e.g., in Cr^{3+}, it is about 10 times stronger than for the lanthanides [1,3,7]. The interactions are expected to be stronger for actinide ions than for lanthanides due to the larger spatial extinction of the $5f^N$ orbitals and weaker shielding by the outer shells. The variation of the electron–phonon coupling strength is reflected in changes of vibronic transitions probabilities and the multiphonon relaxation rate as well as in temperature dependent line shifts and line broadenings. Systematic studies utilizing the last method as a probe, have been recently reported for the lanthanide ions [5,6,8]. It was shown, that the coupling strength increases strongly in the more covalent host lattices [8] and depends also on the kind of the lanthanide ion. The dependence of the last one was explained by (i) the influence of the lanthanide contraction, (ii) the shielding of the $4f$ electrons by the filled outer shells and (iii) the position of the opposite parity states ($4f^{N-1}5d^1$ or charge transfer). The effect of the last factor has been studied for isoelectronic, divalent and trivalent lanthanides ($4f^6$ and $4f^7$) [9]. However, contrary to expectations, the authors have not found significant differences in the temperature-depending line broadening between corresponding divalent and trivalent ions. It indicates, that the position of the opposite parity state is not the main factor affecting the electron–phonon coupling strength.

Ellens et al. [10] have measured the temperature line broadening of U^{3+} and Nd^{3+} ions in K_2LaCl_5 single crystals and have compared the obtained $\bar{\alpha}$ electron–phonon coupling strength parameters. The authors have observed a larger electron–phonon coupling for the actinide ion, however, they have obtained also considerably different values of the $\bar{\alpha}$ parameter for various

*Corresponding author. Fax: +48-71-222-348.
E-mail address: jd@wchuwr.chem.uni.wroc.pl (J. Drożdżyński).

0022-4596/03/$ - see front matter © 2003 Elsevier Science (USA). All rights reserved.
doi:10.1016/S0022-4596(03)00089-6

transitions of the same ion. Since the values of the $\bar{\alpha}$ parameter strongly depend on the investigated transition, a reliable comparison of the results can be obtained from considerations of the same levels, only. For the U^{3+} and Nd^{3+} ions in the K_2LaCl_5 host crystal the $\bar{\alpha}$ parameters have been determined for one analogous transition only, mainly the $^4I_{9/2} \rightarrow {}^4G_{5/2}$ one. This results in part from a more limited range available for the analysis of the U^{3+} f–f bands in the K_2LaCl_5 host, which is due to the appearance of strong f–d bands at an energy as low as 15,300 cm^{-1}, whereas in the $LaCl_3$ host investigated by us, the first f–d transitions are observed at a considerably higher energy of $\sim$21,000 cm^{-1}. This extends the range of analogous U^{3+} and Nd^{3+} transitions for which temperature induced line broadening could be measured and the determined EP coupling parameters could be compared. Moreover, by comparison with the values obtained for the K_2LaCl_5 host the influence of the position of the opposite parity states and changes in covalency on the broadening of the U^{3+} lines could be checked. In order to compare the influence of covalency we have also performed similar measurements for U^{3+} doped $LaBr_3$ single crystals. The strength of the electron–phonon coupling, determined from the temperature line broadening was compared with those obtained from temperature induced line shifts.

2. Experimental details

The U^{3+}(0.5 mol%):$LaCl_3$, Nd^{3+}(0.5 mol%):$LaCl_3$ and U^{3+}(0.5 mol%):$LaBr_3$ single crystals were grown in silica ampoules by the Bridgman–Stockbarger method. $LaCl_3$, $LaBr_3$ and $NdCl_3$ were synthesized from the appropriate oxides by the ammonium halogenide route [11] and sublimed under high vacuum. UCl_3 and UBr_3 were prepared according to the method reported in Refs. [12] and [13], respectively. Approximately $5 \times 5 \times 0.5\,mm^3$ pieces of single crystals have been cut out from a bulk crystal and polished under a dry paraffin oil. The absorption spectra of unoriented samples were recorded on a Cary 5 NIR-Vis–UV spectrophotometer. The temperature of the samples was varied between 7 K and room temperature with an Oxford Instruments cryostat and the Lake Shore Autotuning Temperature Controller.

3. Theory

Measurements of temperature-induced line broadening and line shifts were chosen as a method for determination of the EP coupling strength. At elevated temperatures the lifetimes of both the initial and final level of a transition are shortened due to the phonon-induced relaxation process. This results in a larger uncertainty in energy and broadening of a spectral line [5].

The experimentally observed line width is a sum of the temperature independent inhomogeneous line width E^{Inh}, which is caused by strains and defects in the lattice, and the temperature dependent, homogeneous line width, E^{Hom}:

$$\bar{E}(T) = E^{\mathrm{Inh}} + E^{\mathrm{Hom}}.$$

Various relaxation processes can be responsible for the shortening of the lifetime, which contribute to the homogenous line width, but the most important ones are the one-phonon emission and absorption process (the direct process) and the Raman two-phonon process. The contribution of the direct process is relatively large at low temperatures, but at higher temperatures the Raman process dominates. It was shown [5,14], that the negligence of the direct process can introduce a considerable error in the determination of the EP coupling parameters. However, it was also concluded [5] that even in such case the order of magnitude of the $\bar{\alpha}$ parameter is retained. Moreover, the evaluation of the direct process is a difficult task because of several one-phonon emissions and absorptions, which must be taken into account. A fit to an equation which includes a number of unknown parameters for both the direct and Raman process could result in obtaining less reliable parameter values than those received from a fit to the Raman equation, only. Hence, in a study where one does not intends to compare the absolute but the relative EP coupling strength the contribution from the direct process may be neglected.

Thus, the line broadening can be fitted to the simplified Eq. (1) containing only the inhomogeneous broadening and temperature depending broadening due to the Raman two-phonon process [1,15]:

$$\begin{aligned}\bar{E}(T) &= E^{\mathrm{Inh}} + E^{\mathrm{R}}(T) \\ &= E^{\mathrm{Inh}} + \bar{\alpha}\left(\frac{T}{T_{\mathrm{D}}}\right)^7 \int_0^{T_{\mathrm{D}}/T} \frac{x^6 e^x}{(e^x-1)^2}\,dx, \end{aligned} \quad (1)$$

where $x = \hbar\omega/kT$ and ω is the phonon frequency. The Debye temperature T_{D} is equal to $T_{\mathrm{D}} = \hbar\omega_{\text{cut-off}}/k$ and corresponds to the effective maximum phonon energy. In the Debye approximation the phonon density scales as ω^2 and then drops to zero at the phonon cut-off frequency $\omega_{\mathrm{cut-off}}$.

The thermal shift of a given transitions is due to stationary effects of the phonon–ion interaction and it is assumed to be the algebraic sum of the shifts of the two levels involved in the transitions. The line shift $E(T)$ may be fitted to the Raman two-phonon process described by Eq. (2) [1,15]:

$$E(T) = E(0) + \alpha\left(\frac{T}{T_{\mathrm{D}}}\right)^4 \int_0^{T_{\mathrm{D}}/T} \frac{x^3}{e^x - 1}\,dx, \quad (2)$$

where x and T_D are defined as in Eq. (1), and the position of the line at 7 K was assumed as $E(0)$. Throughout this paper the symbols $\bar{\alpha}$ and α for the electron coupling parameters derived from line broadening and line shift measurements will be used, respectively. According to Eqs. (1) and (2) the symbol $\bar{E}(T)$ refer to the line width and $E(T)$ to the line position at a given temperature.

4. Results and discussion

4.1. Line broadening

The measurements were performed for a number of sufficiently well-isolated transitions in 4000–21,000 cm^{-1} energy range, so that the determination of the line widths could be accomplished in 7–300 K temperature range. However, due to a strong broadening some lines could not be followed in the whole temperature range. Wherever possible, we have tried to measure the same transitions for all investigated compounds. The assignment of the transitions is the same as in Ref. [16–18].

Fig. 1 presents the absorption spectra for the $^4I_{9/2} \rightarrow {}^4F_{9/2}$ transitions of the Nd^{3+}:$LaCl_3$, U^{3+}:$LaCl_3$ and U^{3+}:$LaBr_3$ single crystals at 7 and 210 K. The full-width at half-maximum (FWHM) for the two presented lines of the Nd^{3+} ions are equal to 1.3 and 1.1 cm^{-1} at 7 K and 6.6 and 6.4 cm^{-1} at 210 K. For U^{3+}:$LaCl_3$ the corresponding values are equal to 1.4 and 1.5 cm^{-1} for low temperatures and 10.5 and 9.8 cm^{-1} for 210 K, respectively, while those of U^{3+}:$LaBr_3$ are equal to 1.1 and 1.2 cm^{-1}, and 12.9 and 11.8 cm^{-1}. Thus, one may notice only small differences in the inhomogeneous line width, which indicates that strains and defects in the $LaCl_3$ and $LaBr_3$ lattices are similar. Fig. 2 presents the transitions from the $^4I_{9/2}$ level to two Stark components of the $^4G_{7/2}$ multiplet for the three studied crystals. The relation between the line widths is similar as for the $^4I_{9/2} \rightarrow {}^4F_{9/2}$ transitions. The same holds true for all investigated transitions. At elevated temperatures the width of the lines increases in the series Nd^{3+}:$LaCl_3$ $< U^{3+}$:$LaCl_3$ $< U^{3+}$:$LaBr_3$.

The line widths at 15, 11 and 10 different temperatures between 7 and 280 K were determined by a fit of the spectral profiles with the Voigt type of function, a convolution of the Lorentzian and Gaussian types of the formula:

$$y = y_0 + A\left(\frac{2m_u}{\pi}\frac{w}{4(x-x_0)^2+w^2} + (1-m_u)\frac{\sqrt{4\ln 2}}{w\sqrt{\pi}}e^{4\ln 2(x-x_0)^2/w^2}\right),$$

for U^{3+}:$LaCl_3$, Nd^{3+}:$LaCl_3$ and U^{3+}:$LaCl_3$, respectively. The temperature-dependent FWHM data were then fitted to the Raman two-photon process according

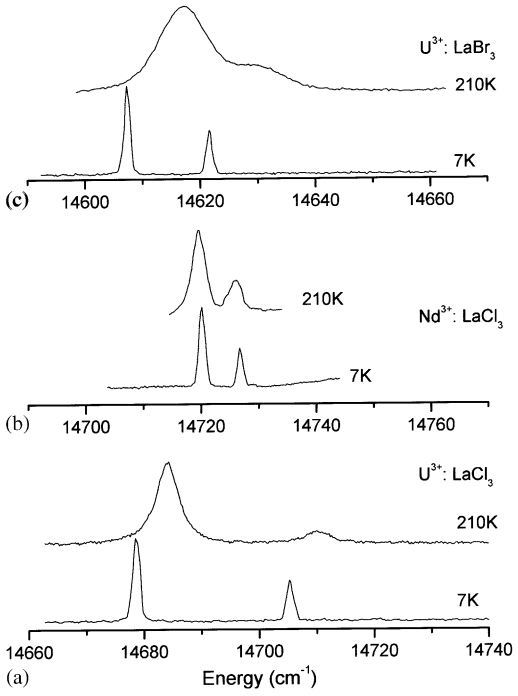

Fig. 1. Absorption spectra of U^{3+}:$LaCl_3$ (a), Nd^{3+}:$LaCl_3$ (b) and U^{3+}:$LaBr_3$ (c) in the $^4I_{9/2} \rightarrow {}^4F_{9/2}$ transition range at 7 and 210 K. The x-axis scale is the same for all spectra.

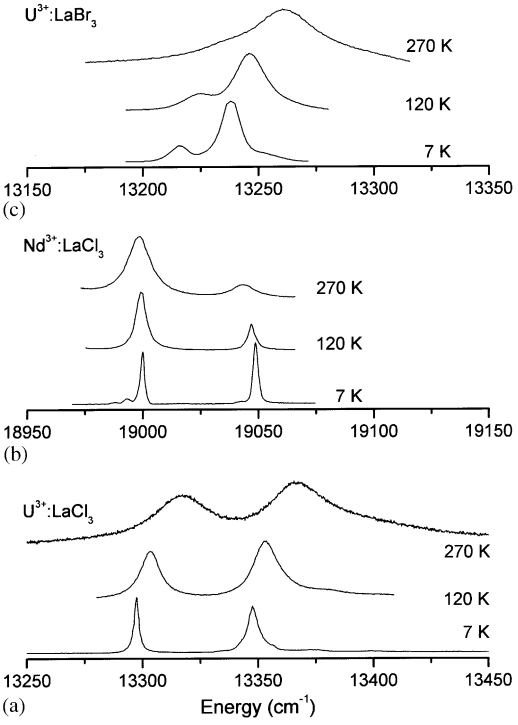

Fig. 2. Absorption spectra of U^{3+}:$LaCl_3$ (a), Nd^{3+}:$LaCl_3$ (b) and U^{3+}:$LaBr_3$ (c) in the $^4I_{9/2} \rightarrow {}^4G_{7/2}$ transition range at 7, 120 and 270 K. The x-axis scale is the same for all spectra.

to the Eq. (1). The accuracy of the fit was given by the σ deviation defined as: $\sigma = \sum_i |\mathrm{Dev}(E(T))| / \sum_i E(T)$, where $Dev(E(T)) = E(T)_{\mathrm{exp}} - E(T)_{\mathrm{calc}}$.

An important factor affecting the *EP* coupling parameters is the Debye temperature. In the absorption or emission spectra of U^{3+} in $LaCl_3$ and $LaBr_3$ for some transitions, vibronic sidebands were observed. Detailed studies of lattice vibrations in the $LaCl_3$ and $LaBr_3$ crystals were reported in Ref. [19]. However, the presented phonon spectra do not follow the ω^2 dependence of the Debye model. The assumption, that the cut-off frequency for the chloride and bromide lattices are equal to the energy of the highest phonon (250 and 185 cm^{-1}, respectively), leads to the Debye temperature of about 360 K for $LaCl_3$ and 265 K for $LaBr_3$. It was found however, that a better fit of the experimentally observed temperature dependence of the line widths was obtained for lower temperatures than those calculated from the cut-off frequency [20–22]. This question was discussed in more detail in Ref. [5]. In the analysis of the Nd^{3+} and U^{3+} doped K_2LaCl_5 [10] single crystals the Debye temperature of 200 K was chosen. In this study we have therefore assumed for the $LaCl_3$ the same value, which enables a comparison of the results obtained for these two host crystals. The somewhat arbitrary choice of T_D may change the absolute value of $\bar{\alpha}$, but not the relations among the parameters. Thus for comparison purposes of different ions in the same type of lattice with a similar phonon energy the choice of the T_D temperature seem not to be very significant.

For the U^{3+} and Nd^{3+} ions in $LaCl_3$ the $\bar{\alpha}$ coefficient was determined by the least-square adjustment of the experimental and calculated points. The values for E^{inh} are the experimental line widths at 7 K. The fits to the temperature-dependent line widths are shown in Fig. 3 and 4 for the U^{3+} and Nd^{3+} ions, respectively. The determined $\bar{\alpha}$ parameters are listed in Tables 1 and 2 along with the values of the line widths at 7 K (E^{Inh}) and the temperature line broadening values ($\Delta\bar{E}(T)$).

The $\bar{\alpha}$ parameters depend strongly on a particular transition, which is probably connected with the direct process. The direct process considerably depends on the energy levels structure and was omitted in our theoretical model. For U^{3+} in $LaCl_3$ the EP coupling parameters remain in a relatively large range between 16 and 86 cm^{-1}. A narrower range, between 16 and 40 cm^{-1} was observed for Nd^{3+}.

Comparing the results obtained for the $LaCl_3$ host crystal with those reported for K_2LaCl_5 [10] one can conclude that the electron phonon coupling is much stronger for the last one. For K_2LaCl_5 the $\bar{\alpha}$ values were reported to be in the 88–200 cm^{-1} and 41–71 cm^{-1} range for U^{3+} and Nd^{3+}, respectively. For U^{3+} in K_2LaCl_5, similarly as for U^{3+} in $LaCl_3$, the largest $\bar{\alpha}$ value was obtained for the $^4G_{7/2}$ multiplet. This is in accordance

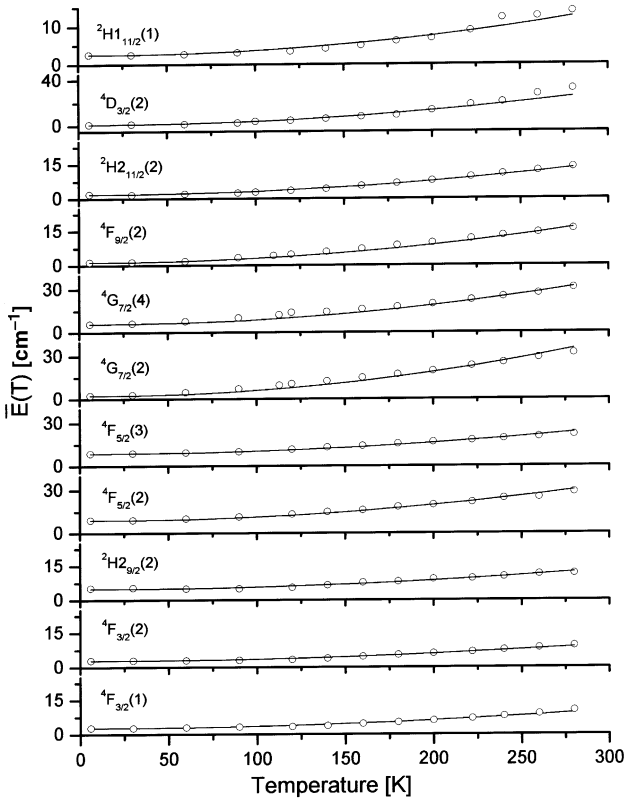

Fig. 3. The line widths of transitions from the $^4I_{9/2}$ ground level to selected crystal-field levels of U^{3+}:$LaCl_3$ as a function of temperature: $^4I_{9/2} \rightarrow {}^4F_{3/2}(1)$, $^4I_{9/2} \rightarrow {}^4F_{3/2}(2)$, $^4I_{9/2} \rightarrow {}^2H2_{9/2}(2)$ etc. Numbers in parenthesis indicate the sequence of appearance of the crystal-field levels, starting with that of lowest energy within the appropriate $^{2S+1}L_J$ multiplet. The circles represents the experimental data and the solid curve is the fit to Eq. (1) for the Raman process.

with the statement that the vibronic side bands, which accompany the absorption transitions to the $^4G_{7/2}$ state are usually the strongest ones. Two factors can contribute to the observed differences of the EP coupling in these two chloride host crystal: the covalency of the lattice and the position of the opposite parity states [15]. In the absorption spectra of U^{3+} in K_2LaCl_5 the $5f^26d^1$ states are observed at energy as low as 15,300 cm^{-1}, i.e., at an about 7000 cm^{-1} lower energy than that in $LaCl_3$. However, it was shown [7] that in the case of divalent lanthanides the low energy of the opposite parity *f–d* states does not significantly influence the temperature dependent line broadening and that the values of the $\bar{\alpha}$ parameters were similar to those obtained for isoelectronic trivalent ions, for which these states are at considerably higher energy. Moreover, the higher positioned nf^{N} levels (with an energy closer to the opposite parity states) should be somewhat broader, but we did not notice such tendency. Additionally, for Nd^{3+}, for which the $4f^25d^1$ states are observed at a high energy the difference in their relative position in $LaCl_3$ and K_2LaCl_5 would be too small to account for a factor of two larger electron–phonon

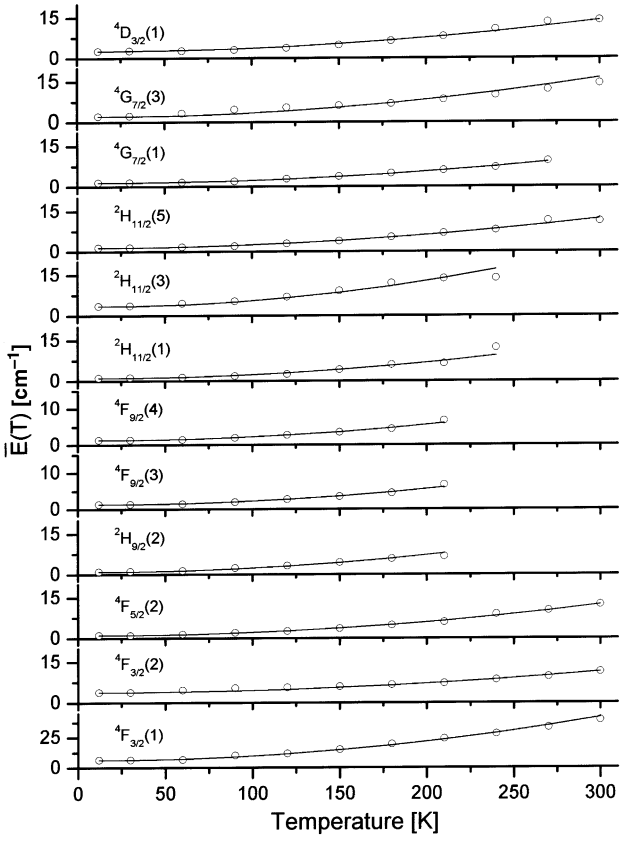

Fig. 4. The line widths of transitions from the $^4I_{9/2}$ ground level to selected crystal-field levels of Nd^{3+}:$LaCl_3$ as a function of temperature: $^4I_{9/2}\rightarrow{}^4F_{3/2}(1)$, $^4I_{9/2}\rightarrow{}^4F_{3/2}(2)$, $^4I_{9/2}\rightarrow{}^4F_{5/2}(2)$ etc. Numbers in parenthesis indicate the sequence of appearance of the crystal-field levels, starting with that of lowest energy within the appropriate $^{2S+1}L_J$ multiplet. The circles represent the experimental data and the solid curve is the fit to Eq. (1) for the Raman process.

coupling constant. Thus the La–Cl (U–Cl) distances seem to be the main factor influencing the EP coupling strength in the K_2LaCl_5 (d(La–Cl) = 2.77–2.88 Å, [23]) and $LaCl_3$ (d(La–Cl) = 2.95–2.954 Å, [24]) host. They are considerably shorter in K_2LaCl_5 which results in a stronger interaction of the ions substituting for La with the Cl^- ligands which leads to an increase of covalency. This is reflected by a stronger CF affecting the ions in K_2LaCl_5. The CF strengths may be compared by the N_v scalar parameter [25]:

$$N_v = \left[\sum_{k,q}(B_q^k)^2\frac{4\pi}{(2k+1)}\right]^{1/2},$$

which is equal to 2144 and 3069 cm^{-1} for U^{3+}:$LaCl_3$ [16] and U^{3+}:K_2LaCl_5 [26], respectively.

From a comparison of the results obtained for U^{3+} and Nd^{3+} in $LaCl_3$ one can conclude, that the EP coupling strength is markedly larger for U^{3+}, although the difference is smaller than the one reported for the K_2LaCl_5 host. For both ions the smallest and almost the same $\bar{\alpha}$ value was obtained for the $^4F_{9/2}\rightarrow{}^4F_{3/2}$ transitions. However, such simple relations are not observed among the other transitions. Moreover, different values were obtained for transitions to Stark levels of the same multiplets. Since the analogous $S'L'J'$ multiplets of the U^{3+} and Nd^{3+} ions are at different positions on the energetic diagram, it seems, that the obtained $\bar{\alpha}$ parameters strongly depend on the energy level structure in the vicinity of the level under consideration. The better shielding of the $4f^3$ electrons by the outer filled shells and the larger spatial extent of the $5f^3$ wavefunction as well as the energetic position of

Table 1
Electron–phonon coupling parameters for various transitions in U^{3+}:$LaCl_3$, determined from the fit of experimentally observed temperature-induced line broadening to Eq. (1)

	Transition[a]	Energy (cm^{-1})	$\Delta\bar{E}(T)$ (K)[b]	$\bar{\alpha}$ (cm^{-1})	E^{Inh} (cm^{-1})	σ[c]
1[d]	$^4I_{9/2}\rightarrow{}^4F_{3/2}(1)$	7081	7.7	17	2.8	0.05
2	$^4I_{9/2}\rightarrow{}^4F_{3/2}(2)$	7099	6.4	16	2.9	0.05
3	$^4I_{9/2}\rightarrow{}^2H2_{9/2}(2)$	9446	6.3	19	4.9	0.04
4	$^4I_{9/2}\rightarrow{}^4F_{5/2}(2)$	9889	19.6	55	9.0	0.04
5	$^4I_{9/2}\rightarrow{}^4F_{5/2}(3)$	9969	12.8	38	8.8	0.04
6	$^4I_{9/2}\rightarrow{}^4G_{7/2}(2)$	13,294	22.9	86	2.5	0.14
7	$^4I_{9/2}\rightarrow{}^4G_{7/2}(4)$	13,344	18.9	67	5.9	0.11
8	$^4I_{9/2}\rightarrow{}^4F_{9/2}(2)$	14,675	11.5	39	1.4	0.07
9	$^4I_{9/2}\rightarrow{}^2H2_{11/2}(2)$	15,422	10.7	30	1.9	0.05
10	$^4I_{9/2}\rightarrow{}^4D_{3/2}(2)$	17,536	9.6	57	2.4	0.06
11	$^4I_{9/2}\rightarrow{}^2H1_{11/2}(1)$	19,753	10.7	26	2.6	0.11
12	$^4I_{9/2}\rightarrow{}^2D1_{5/2}(2)$	20,204	9.1[e]	81	2.9	0.10

[a] Transition assignments are taken from Ref. [17]. Numbers in parentheses labels the subsequent crystal field components, starting from that of the lowest energy, within a given excited multiplet $^{2S+1}L_J$.
[b] Difference of the line width at 280 and 7K.
[c] σ deviation defined as $\sigma = \sum_i |\mathrm{Dev}(E(T))|/\sum_i E(T)$, where $\mathrm{Dev}(E(T)) = E(T)_{\mathrm{exp}} - E(T)_{\mathrm{calc}}$.
[d] Numbers in this column label the transitions and correspond to numbers on the x-axis in Fig. 6.
[e] Value derived for the 7–180 K temperature range.

Table 2
Electron–phonon coupling parameters for various transitions in Nd^{3+}:$LaCl_3$, determined from the fit of experimentally observed temperature-induced line broadening to Eq. (1)

Transition[a]	Energy (cm^{-1})	$\Delta\bar{E}(T)$ (K)[b]	$\bar{\alpha}$ (cm^{-1})	E^{Inh} (cm^{-1})	σ[c]
$^4I_{9/2}\rightarrow{}^4F_{3/2}(1)$	11,424	5.7	16	19	0.03
$^4I_{9/2}\rightarrow{}^4F_{3/2}(2)$	11,454	7.5	17	24	0.09
$^4I_{9/2}\rightarrow{}^4F_{5/2}(2)$	12,480	11.3	26	1.1	0.04
$^4I_{9/2}\rightarrow{}^2H_{9/2}(2)$	12,557	5.6[d]	32	1.0	0.07
$^4I_{9/2}\rightarrow{}^4F_{9/2}(3)$	14,715	5.3[d]	22	1.3	0.05
$^4I_{9/2}\rightarrow{}^4F_{9/2}(4)$	14,722	11.1[d]	29	1.1	0.14
$^4I_{9/2}\rightarrow{}^2H_{11/2}(1)$	15,907	9.7	25	1.5	0.05
$^4I_{9/2}\rightarrow{}^2H_{11/2}(3)$	15,948	7.9	21	1.44	0.03
$^4I_{9/2}\rightarrow{}^2H_{11/2}(5)$	15,961	13.9	29	1.8	0.08
$^4I_{9/2}\rightarrow{}^4G_{7/2}(1)$	18,994	12.1	32	2.1	0.13
$^4I_{9/2}\rightarrow{}^4G_{7/2}(3)$	19,042	11.2	26	2.6	0.06
$^4I_{9/2}\rightarrow{}^4D_{3/2}(1)$	27,973	16.5	40	3.1	0.04

[a] Transition assignments are taken from Ref. [18]. Numbers in parentheses labels the subsequent crystal field components, starting from that of the lowest energy, within a given excited multiplet $^{2S+1}L_J$.
[b] Difference of the line width at 280 and 7 K.
[c] σ deviation defined at footnote (c) of Table 1.
[d] Value derived for the 7–210 K temperature range.

the opposite parity state seem to be responsible for the differences in the $\bar{\alpha}$ values of the U^{3+} and Nd^{3+} ions.

The two photon Raman process can take place by two different mechanisms: the extrinsic and intrinsic Raman process [15]. In the extrinsic Raman two phonon process one phonon is absorbed and one is emitted simultaneously by means of the first-order term of the EP interaction for the two phonons. The matrix element for the transition probability of this process is inversely proportionate to the energy differences between the initial and an intermediate state involved in the phonon absorption and emission. For lanthanide ions it is generally accepted, that the intermediate states are states of opposite parity, because the transition probability for a process involving an opposite parity state is assumed (based on *ms* vs. *ns* lifetimes for *f–f* and *f–d* transitions) to be 10^6 times higher than that for a process involving the $4f^N$ states [7]. However one may not rule out that the nearby $4f^N(5f^N)$ states instead those of $4f^{N-1}6d^1(5f^{N-1}6d^1)$ are involved in the extrinsic process.

In the intrinsic Raman process the phonons are scattered by the second-order term of the electron–phonon interaction and an intermediate state is not involved in this process. For the Nd^{3+} ions the opposite parity states are distinctly far from the investigated *f–f* transitions at an energy of $\sim$46,000 cm^{-1} whereas for the U^{3+} ions the *f–d* transitions are observed at a considerably lower energy of about 21,000 cm^{-1}. For the U^{3+} ions the energy differences between the investigated transitions and the first *f–d* state are of the 1,000–14,000 cm^{-1} magnitude. If one assumes that the extrinsic Raman process involving opposite parity state, was responsible for the line broadening one should observe a larger electron–phonon coupling for levels positioned closer to the $5f^26d^1$ states. In the spectrum of U^{3+}:$LaCl_3$ for the closest multiplet, the $^2D1_{5/2}$, one of the largest value of the $\bar{\alpha}$ parameters was obtained (however it was not proved by the line shift analysis, see next section) but for the next one, the $^2H1_{11/2}$, positioned at only 500 cm^{-1} lower energy one gets a relatively small $\bar{\alpha}$ value, which may indicate that the positions of the opposite parity states do not influence the observed line broadening. Hence, the extrinsic Raman process through the nearby $5f^3$ states or the intrinsic Raman process can be regarded as the possible broadening mechanism. However, as it was mentioned earlier, the dominant factor responsible for the strength of the EP coupling for the Nd^{3+} and U^{3+} ions is the difference in the spatial extent of the 4*f* and 5*f* wavefunctions as well as the shielding of the 4*f* and 5*f* ions by the outer shells. This is again well illustrated by the difference in the crystal-field strength affecting both ions, expressed by the N_v parameter, which is for U^{3+} of a factor of 2 larger than that for Nd^{3+}. A similar relation is observed for the $\bar{\alpha}$ parameters obtained for both ions.

4.2. Line shifts

An accurate determination of the experimental line widths usually requires the deconvolution of the spectral profile with the Voigt type of function (which is sometimes approximated by the pure Lorentzian one). However in cases were several bands overlap, especially at elevated temperatures it can lead to a considerable uncertainty of the obtained values. Generally, it is more reliable to determine the position of a peak than its width. Moreover, with a temperature change an increase in FWHM shifts of the lines are observed. Therefore we

have decided to compare the $\bar{\alpha}$ parameters obtained for U^{3+} in $LaCl_3$ from the analysis of the line width with those arising from line shifts.

With increasing temperature usually a red shift of spectral lines of Ln^{3+} ions occurs. However, in some cases a shift towards shorter wavelengths (the blue shift) was also observed. For example, for Nd^{3+} in $CaZn_2Y_2Ge_3O_{12}$ a blue shift was observed for the $^4F_{3/2} \rightarrow {}^4I_{9/2}$ transition line and a red shift for the $^4F_{3/2} \rightarrow {}^4I_{11/2}$ one [4].

In this study, we have observed a blue shift of all U^{3+} lines in the $LaCl_3$ crystal with the temperature increase, contrary to the Nd^{3+} ions in the same host in which the red shift dominates. However, it was not a rule for all investigated transitions of the Nd^{3+} ions. For example with a temperature increase the $^4F_{3/2}(2)$ level at 11464 cm^{-1} shifts towards lower wavelength, while the second Stark component of this multiplet moves first towards higher wavelengths and next, at about 150 K back to a lower energy. An opposite tendency was observed for the $^2H_{11/2}$ multiplet, where, with a temperature increase the (1st), (3rd) and (5th) component of the multiplet moved first to a lower and then to higher energy. Such a behavior cannot be easily accounted for by the processes discussed in Section 3 and is probably due to other effects. Besides, the relative population of the crystal field components of the $^4I_{9/2}$ ground multiplet is changed with increasing temperature. This may lead to a line shift which overlaps with the shifts resulted from the EP coupling.

The measured line shifts for the analyzed transitions of the U^{3+} ions are plotted in Fig. 5. The experimental line shifts have been fitted to Eq. (2). The obtained fitting parameters are included in Table 3. The Debye temperature was assumed to be $T_D = 200$ K, similarly as in the analysis of HWMH. Fig. 6 shows the $\bar{\alpha}$ and α parameters derived form the line width and line shift analyses of U^{3+} ions in $LaCl_3$, respectively.

The results of the line shift analysis are in general accordance with those obtained from the line width analysis, although the curve corresponding to the line shift data is somewhat smoother. For both approaches the smallest EP coupling coefficient was obtained for the $^4F_{3/2}$ multiplet, while the largest one for the $^4G_{7/2}$ one. The only significant difference was observed for the $^2D1_{5/2}$ multiplet. Its line shift stays in the range with those observed for the other levels but, contrary to them, it is strongly broadened at room temperatures.

4.3. Comparison of the electron–phonon coupling in U^{3+} doped $LaCl_3$ and $LaBr_3$ single crystals

An analysis of the line width and line shift measurements for the U^{3+} (0.5 mol%):$LaBr_3$ crystal has also been performed but for this host crystal the Debye temperature cannot be evaluated. If one intend to

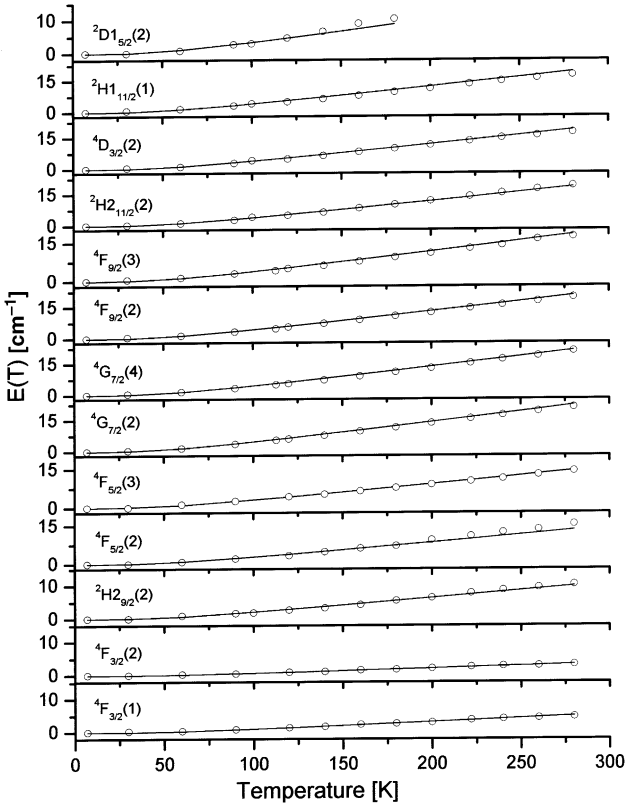

Fig. 5. The line shifts of transitions from the $^4I_{9/2}$ ground level to selected crystal-field levels of U^{3+}:$LaCl_3$ as a function of temperature: $^4I_{9/2} \rightarrow {}^4F_{3/2}(1)$, $^4I_{9/2} \rightarrow {}^4F_{3/2}(2)$, $^4I_{9/2} \rightarrow {}^2H2_{9/2}(2)$ etc. Numbers in parenthesis indicate the sequence of appearance of the crystal-field levels starting with that of lowest energy within the appropriate $^{2S+1}L_J$ multiplet. The circles represent the experimental data and the solid curve is the fit to Eq. (2) for the Raman process.

Table 3
Experimental line shifts and electron–phonon coupling parameters for various transitions in U^{3+}:$LaCl_3$, determined from the fit of experimentaly observed temperature-induced line shifts to Eq. (2)

	Transition[a]	Energy (cm^{-1})	$\delta E(T)$[b]	α (cm^{-1})	σ[c]
1[d]	$^4I_{9/2} \rightarrow {}^4F_{3/2}(1)$	7081	4.3	14	0.05
2	$^4I_{9/2} \rightarrow {}^4F_{3/2}(2)$	7099	3.1	9	0.05
3	$^4I_{9/2} \rightarrow {}^2H2_{9/2}(2)$	9446	10.0	28	0.04
4	$^4I_{9/2} \rightarrow {}^4F_{5/2}(2)$	9889	15.3	37	0.04
5	$^4I_{9/2} \rightarrow {}^4F_{5/2}(3)$	9969	14	40	0.04
6	$^4I_{9/2} \rightarrow {}^4G_{7/2}(2)$	13,294	17.3	62	0.14
7	$^4I_{9/2} \rightarrow {}^4G_{7/2}(4)$	13,344	17	60	0.11
8	$^4I_{9/2} \rightarrow {}^4F_{9/2}(2)$	14,675	16	58	0.07
9	$^4I_{9/2} \rightarrow {}^4F_{9/2}(3)$	14,701	13.9	52	0.06
10	$^4I_{9/2} \rightarrow {}^2H2_{11/2}(2)$	15,422	19	52	0.05
11	$^4I_{9/2} \rightarrow {}^4D_{3/2}(2)$	17,536	6.3	52	0.06
12	$^4I_{9/2} \rightarrow {}^2H1_{11/2}(1)$	19,753	17.6	54	0.11
13	$^4I_{9/2} \rightarrow {}^2D1_{5/2}(2)$	20,204	9.9[e]	45	0.08

[a] Transition assignments are taken from Ref. [17]. Numbers in parentheses labels the subsequent crystal field components, starting from that of the lowest energy, within a given excited multiplet $^{2S+1}L_J$.
[b] Difference of the line position at 280 and 7 K.
[c] σ deviation defined at footnote (c) of Table 1.
[d] Numbers in this column label the transitions and correspond to numbers on the x-axis in Fig. 7.
[e] Value derived for the 7–180 K temperature range.

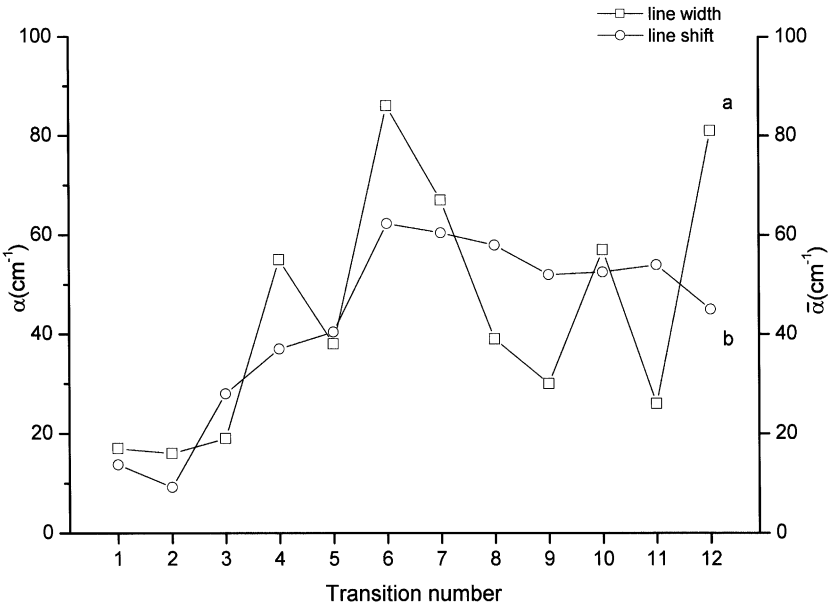

Fig. 6. A comparison of the EP coupling parameters ($\bar{\alpha}$ and α) determined from analysis of the temperature-induced line broadening (a) and line shift (b) for various transitions in U^{3+}:$LaCl_3$. The numbers on the x-axis labels the transitions and correspond to numbers in the first column of Table 1. The line between points is added for better visualization only.

compare the EP coupling strengths for U^{3+} and Nd^{3+} ions in the same host crystal only, the choice of the Debye temperature is not crucial, but it becomes of great importance for a comparison of ions in different lattices, in this case the chloride and bromide lattices. For $LaBr_3$ a lower Debye temperature is expected due to the lower cut-off energy of the lattice. Some vibronic lines were observed in the $LaBr_3$ spectra, but they do not follow the Debye relation and therefore we were not in a position to determine the true relations between the T_D temperatures for the two host crystals. Since the EP coupling parameters strongly depend on the chosen Debey temperature and it was not possible to obtain a true relation between the parameters of the Nd^{3+} and U^{3+} ions in the $LaCl_3$ and $LaBr_3$ host crystals we have performed, instead, a comparison of the magnitudes of the absolute increase of the line width and line shifts between 5 and 280 K (Fig. 7). We have found that only for the $^4F_{5/2}$ (2) level the increase in the line width is smaller for the bromide than for chloride host, as well as that for all investigated transitions the blue shift is larger in the $LaBr_3$ host. Hence, one may conclude, that the electron–phonon coupling is stronger in the bromide host. In $LaBr_3$ the uranium–ligand distances are larger and in result of this the U^{3+} ions in $LaBr_3$ are affected by a weaker crystal-field. Since in this crystal the position of the first f–d states at $\sim 20{,}000\,cm^{-1}$ is only slightly lower then that in the chloride crystal, the main factor which can account for the observed differences in the EP coupling is a the difference in covalency of both hosts. In a more covalent host, there exists a stronger

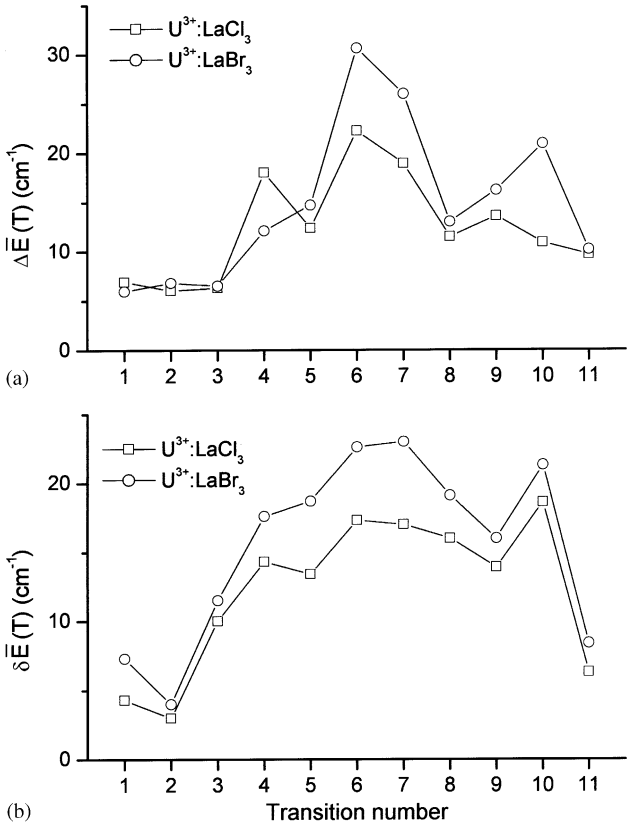

Fig. 7. A comparison of the absolute increase of the line width- $\Delta\bar{E}(T)$ (a) and line shift $\delta E(T)$ (b) between 7 K and room temperature for various transitions of U^{3+} in $LaCl_3$ (circles) and in $LaBr_3$ (squares). The numbers on the x-axis labels the transitions and correspond to the numbers in the first column of Table 3. The line between the points is added for better visualization only.

overlap between the wavefunctions of the metal and the ligands and, as a result of this, a stronger EP coupling is expected. A similar influence of the host lattice covalency has been earlier observed also for some lanthanide ions [8] and for Cr^{3+} doped garnets [7].

Further investigations of U^{3+} ions in two somewhat only different sites of the RbY_2Cl_7 host crystal are presently being conducted in order to examine the influence of small differences in the surroundings of central ion on the EP coupling strength.

5. Conclusions

The temperature induced line broadening and line shifts were chosen as a method for the determination of the electron–phonon coupling parameters. The values of the parameters have been determined for U^{3+}:$LaCl_3$ and Nd^{3+}: $LaCl_3$ single crystals by a fit of the experimentally observed line widths to a equation containing the temperature dependent broadening due to the Raman two-phonon process. The obtained parameters are smaller than those determined for the ions in the K_2LaCl_5 host crystal. This effects from the shorter M–Cl distances in $LaCl_3$ caused stronger interactions with the chloride ligands and led to an increase of covalency. The position of the opposite parity states seem to be of minor importance. The $\bar{\alpha}$ parameters are markedly larger for U^{3+} in $LaCl_3$ than those for Nd^{3+} in the same lattice. The main factor responsible for this difference is the less effective shielding of the $5f$ electrons by the filled $6s^2$ and $6p^2$ shells as well as the larger spatial extent of the $5f$ orbitals. Contrary to Nd^{3+}, for the absorption lines of U^{3+} ions in the $LaCl_3$ host crystal, with a temperature increase a blue shift is observed. A good correlation has been found among the EP coupling parameters obtained for U^{3+}:$LaCl_3$ from an analysis of the line widths and of those determined from temperature-induced line shifts. Due to a problematic Debye temperature of the $LaBr_3$ lattice we did not attempt to determine the EP coupling parameters in this host crystal. Instead the magnitudes of the absolute increase in the line width and line shifts for U^{3+} ions in the chloride and bromide hosts between 7 K and room temperature have been compared. The EP coupling is stronger for U^{3+} in $LaBr_3$ as compared to the $LaCl_3$ host which mainly results from a larger covalency of the last one.

The interpretation of the EP coupling is a difficult task and the obtained results cannot be considered as quite satisfactory. This mainly results from the fact that various, still not well understood processes may contribute to the experimentally observed temperature-dependent line broadening and line shifts. The most important ones are the one-phonon direct process and the Raman two-phonon process. However, in cases when only a limited number of experimental data is available, which is for example the case of the U^{3+} ions, the contribution from the direct process cannot be evaluated and a simplified equation containing only the temperature broadening due to the Raman two-phonon process is applied. The importance of the direct process may be suggested by the fact, that the $\bar{\alpha}$ parameters obtained from the fit to Eq. (1) depend strongly on a particular transition. The absolute value of the $\bar{\alpha}$ parameter cannot be determined, but hopefully the order of magnitude should be retained. Another important factor which is making the determination of the absolute values of the alpha parameter impossible is the Debye temperature, which must be often chosen to some degree arbitrarily. Thus the EP coupling parameters, which results from the analysis with the above assumption, can be used for comparison purposes only, preferably for different ions in the same type of lattice, with similar phonon energy and CF strength. On the other hand the obtained parameters are reflecting the differences in M–Cl distances, the shielding of the $4f$ and $5f$ electrons and the host covalency. Similarly as other authors, we have not observed a clear influence of the positions of the opposite parity states on line broadening.

Acknowledgment

This work was supported by the Polish Committee for Scientific Research within the Project No.7TO9A080 20 (4579/PB/WCH/01), which is gratefully acknowledged.

References

[1] T. Kushida, Phys. Rev. 185 (1969) 500.
[2] W.M. Yen, W.C. Scott, A.L. Schawlow, Phys. Rev. 136 (1964) A271.
[3] X. Chen, B. Di Bartolo, J. Lumin. 54 (1993) 309.
[4] D.K. Sardar, R.M. Yow, Opt. Mater. 10 (1998) 191.
[5] A. Ellens, H. Andres, A. Meijerink, G. Blasse, Phys. Rev. B 55 (1997) 173.
[6] A. Ellens, H. Andres, M.L.H. ter Heerdt, R.T. Wegh, A. Meijerink, G. Blasse, Phys. Rev. B 55 (1997) 180.
[7] A.P. Vink, A. Meijerink, J. Phys. Chem. Solids 61 (2000) 1717.
[8] A. Meijerink, G. Blasse, J. Sytsma, C. de Mello Donega, A. Ellens, Acta Phys. Pol. A 90 (1996) 109.
[9] A.P. Vink, M.A. Reijme, A. Meijerink, J. Lumin. 92 (2001) 189.
[10] A. Ellens, K. Krämer, H.U. Güdel, J. Lumin. 76&77 (1998) 548.
[11] G. Meyer, Inorg. Synth. 25 (1989) 146.
[12] J. Drożdżyński, Polyhedron 7 (1988) 167.
[13] E. Zych, J. Drożdżyński, Polyhedron 9 (1990) 2175.
[14] J.T. Gourlay, Phys. Rev. B 5 (1972) 22.
[15] B. Henderson, G.F. Imbusch, Optical Spectroscopy of Inorganic Solids, Oxford University Press, Oxford, 1989.
[16] W.T. Carnall, Systematic analysis of the spectra of trivalent actinide ions in D_{3h} site symmetry, ANL Report89/39, Argon National Laboratory, IL, USA.
[17] M. Karbowiak, J. Drożdżyński, M. Sobczyk, J. Chem. Phys. 117 (2002) 2800.

[18] H.M. Crosswhite, H. Crosswhite, F.W. Kaseta, R. Sarup, J. Chem. Phys. 64 (1976) 1981.
[19] I. Richman, R.A. Sattte, Y. Wong, J. Chem. Phys. 39 (1963) 1833.
[20] T. Kushida, Phys. Rev. 185 (1969) 500.
[21] D.E. McCumber, M.D. Sturge, J. Appl. Phys. 34 (1963) 1682.
[22] J. Danko, D. Pacheco, B. Di Bartolo, Phys. Status Solidi A 63 (1981) K31.
[23] M. Wickleder, University at Cologne, Germany, private information.
[24] T. Schleid, G. Meyer, L.R. Morss, J. Less-Common Met. 132 (1997) 69.
[25] F. Auzel, O.L. Malta, J. Phys. 44 (1983) 201.
[26] M. Karbowiak, N. Edelstein, Z. Gajek, J. Drożdżyński, Spectrochim. Acta A 54 (1998) 2035.